Photonic band gaps tuned by atomic configurations in binary-compound photonic crystals

S. Nojima and T. Mizoi
Graduate School of Integrated Science, Yokohama City University, 22-2 Seto, Kanazawa, Yokohama, Kanagawa 236-0027, Japan
(Received 11 January 2005; published 31 May 2005)

We report photonic crystals with two different rod atoms in the unit cell, the relative configuration of which is carefully regulated to optimize the photonic band structures (two-dimensional binary-compound photonic crystals). The photonic band gaps between any bands are found to be tuned by introducing the second atom at an appropriate position in the unit cell. In particular, by elaborately searching for the optimal position of the second atom, we can determine the atomic configurations that maximize the photonic band gaps.

DOI: 10.1103/PhysRevB.71.193106 PACS number(s): 42.70.Qs, 78.67.−n, 42.70.Nq

Periodic dielectric structures, which we call photonic crystals (PCs), have attracted much interest in recent years.[1,2] The principal feature exhibited by the PCs is the creation of photonic bandgaps, i.e., the frequency regions in which all optical modes are forbidden to exist. Since most applications of the PCs rely on the existence of photonic band gaps, it is desirable that we could design the PC structures to create the photonic band gaps with a desired width at a desired frequency position. The large photonic band gaps will increase the tolerance for designing PC optical devices and also augment the anomalous dispersions near the photonic band edges.[3] The creation of large photonic band gaps therefore has been one of the continued primary interests in theoretical and experimental investigations. A variety of theoretical approaches have been carried out for searching for large photonic band gaps.[4–12] As a natural consequence of the consideration on the gap formation mechanisms, the approach conducted first was to find the optimums for the crystal lattice types, the filling factor of atoms in the unit cell, and the dielectric-constant contrast between atoms and background.[4] The introduction of anisotropy into the PCs, such as using the anisotropic dielectric constants[5] and the dielectric constants that are different between two light-polarizations,[6] has also shown to be useful to tailor the photonic band gaps. The third attempt was to use the double-layered atoms to create photonic band gaps.[7,8] The symmetry reduction of the PC structures was also found to be efficient to tune the photonic band gaps, because it lifted the degeneracy of highly symmetric points in the band structures and as a result enlarged the photonic band gaps in some cases.[9–12] In this attempt, the symmetry reduction was carried out either by introducing another atom at the center of the unit cell[9–11] or by twisting the atoms.[12]

This paper reports binary-compound photonic crystals that contain two different atoms in the unit cell. In this PC, the relative configurations of two atoms in the unit cell are carefully adjusted so that the photonic band structures be optimized. This is obviously an analog of the binary-compound semiconductors (e.g., GaAs), the atoms of which, however, have a certain fixed configuration because of the natural crystals. In contrast, the PCs that are artificial crystals make it possible to place atoms at arbitrary positions. Although this proposal is similar to the last attempt mentioned in the preceding paragraph, it has an advantage that enables us to more precisely design the band structures by utilizing additional arbitrary parameters (the second atom position). To the authors' knowledge, this kind of approach has not been reported, and hence it will prove useful in designing photonic band-gaps of a variety of photonic crystals.

In this report, we consider the two-dimensional (2D) PCs and use the plane-wave expansion method for calculating photonic band structures. Since this method has been reported in many literatures,[13] we here mention it briefly. We focus on the E polarization, for which the electric field $\mathbf{E}$ is parallel to the rod axis, i.e., $\mathbf{E}=[0,0,E_z(\mathbf{r})]$, where $\mathbf{r}=(x,y)$ is the 2D position vector. The electric field $E_z(\mathbf{r})$ can be expanded into the Fourier series of the Bloch type with the expansion coefficients $E_z(\mathbf{G})$. The Maxwell equation for $E_z(\mathbf{r})$ then reduces to the eigenvalue problem for $E_z(\mathbf{G})$

$$\sum_{\mathbf{G}'} |\mathbf{K}+\mathbf{G}||\mathbf{K}+\mathbf{G}'|\varepsilon^{-1}(\mathbf{G}-\mathbf{G}')E_z(\mathbf{G}') = \left(\frac{\omega}{c}\right)^2 E_z(\mathbf{G}), \tag{1}$$

where $\mathbf{K}$ is the Bloch wave vector. Here, the summation extends over all reciprocal lattice points $\mathbf{G}'=n_1\mathbf{b}_1+n_2\mathbf{b}_2$, where $\mathbf{b}_1$ and $\mathbf{b}_2$ are primitive reciprocal lattice vectors, and n_1 and n_2 are arbitrary integers. In Eq. (1), $\varepsilon^{-1}(\mathbf{G})$ is the Fourier transform of the inverse dielectric function $\varepsilon^{-1}(\mathbf{r})$ in the real space and is given by

$$\varepsilon^{-1}(\mathbf{G}) = \varepsilon_b^{-1}\delta_{\mathbf{G},0} + (\varepsilon_{a1}^{-1}-\varepsilon_b^{-1})f_1\frac{2J_1(GR_1)}{GR_1} + (\varepsilon_{a2}^{-1}-\varepsilon_b^{-1})e^{-i\mathbf{G}\cdot\mathbf{P}}f_2\frac{2J_1(GR_2)}{GR_2}, \tag{2}$$

for the binary-compound PC that contains in its unit cell the first rod [radius R_1, dielectric constant ε_{a1}, and filling factor $f_1=\pi(R_1/a)^2$] and the second rod [R_2, ε_{a2}, and $f_2=\pi(R_2/a)^2$] with the background of ε_b. Here, $J_1(x)$ is the first-order Bessel function, and $\mathbf{P}$ indicates the position of the second rod in a unit cell viewed from the first rod at the origin. In this report, the square lattice with primitive lattice vectors of $\mathbf{a}_1=a(1,0)$ and $\mathbf{a}_2=a(0,1)$ is assumed with the reciprocal lattice vectors given by $\mathbf{b}_1=2\pi/a(1,0)$ and $\mathbf{b}_2=2\pi/a(0,1)$, where a is the lattice constant. The material parameters used are $\varepsilon_{a1}=10$ and $\varepsilon_{a2}=15$ and $R_1=0.1a$ and $R_2=0.1a$ for the two rods, and $\varepsilon_b=1$. The frequency eigen-

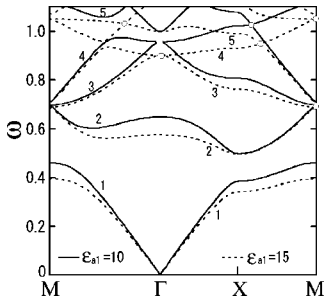

FIG. 1. Photonic band structures for *E*-polarized light in two-dimensional square lattice PCs in the air with a single rod atom in the unit cell with dielectric constants of $\varepsilon_a=10$ (solid line) and $\varepsilon_a=15$ (broken line). Open circles indicate the degenerate points. The angular frequency ω is normalized in units of $2\pi c/a$.

values ω are obtained by diagonalizing the relevant matrices. The study of the eigenvalue convergence revealed that the 49×49 reciprocal lattice points were sufficient to diagonalize the matrices for any configurations of two rod atoms in the unit cell. In all figures in this report, the angular frequency ω is normalized in units of $2\pi c/a$. This report discusses the so-called quality factor of the band gap defined by $Q_{ij}\equiv\Delta\omega_{ij}/\omega_{ij}$, where $\Delta\omega_{ij}=\omega_j-\omega_i$ is the band gap between the two bands with indices i and j ($i<j=i+1$, and ω_i is the top of band i and ω_j is the bottom of band j) and $\omega_{ij}=(\omega_i+\omega_j)/2$ is the middle frequency in the gap. Here, we put $Q_{ij}=0$ when $\omega_i\geqslant\omega_j$, i.e., there is no gap. It is recommended that the readers should look at the results for Q_{ij} (Fig. 2) and those for the band structures (Figs. 1 and 3), and compare them appropriately.

Prior to investigating the effects of atomic configurations on the photonic band gap formation, we first calculated the PCs with a single atom in the unit cell. Figure 1 shows the photonic band diagrams for the PCs with a single atom of $\varepsilon_{a1}=10$ and $R_1=0.1a$ (solid line) and $\varepsilon_{a1}=15$ and $R_1=0.1a$ (dotted line). These atoms are the same elements as those which will be used in the study of the binary-compound PCs. The two diagrams in Fig. 1 are similar to each other because of the difference only in the dielectric constants: the first band gap (the gap between bands 1 and 2) opens while no other band gaps open. Since the rod radius is not optimized, the quality factor Q_{12} of this band gap is not very high: $Q_{12}=0.082$ for the first PC (solid line) and $Q_{12}=0.22$ for the second PC (dotted line). Even by changing the rod radius from 0 to $0.5a$ (the possible maximum value), the 2-3 band gap does not open though the 3-4 and 4-5 band gaps open slightly. The PC with a single atom in the unit cell of the square lattice has the symmetry operations that belong to the C_{4v} point group: their operations are denoted as $(E,C_4,C_4^{-1},C_2,\sigma_x,\sigma_y,\sigma_d',\sigma_d'')$.[14] Owing to the high symmetry of this PC, bands 2 and 3 are still degenerate at M point while other bands 1 and 4 are split off from the original degenerate level (these four bands were degenerate at M point for the free-photon square lattice). The similar situation occurs for the four bands (2 to 5) at Γ point and a new degeneracy occurs at a middle point on the X-M line. These multiple degeneracies appear to make this PC fail to create any band gaps except the 1-2 photonic band gap.

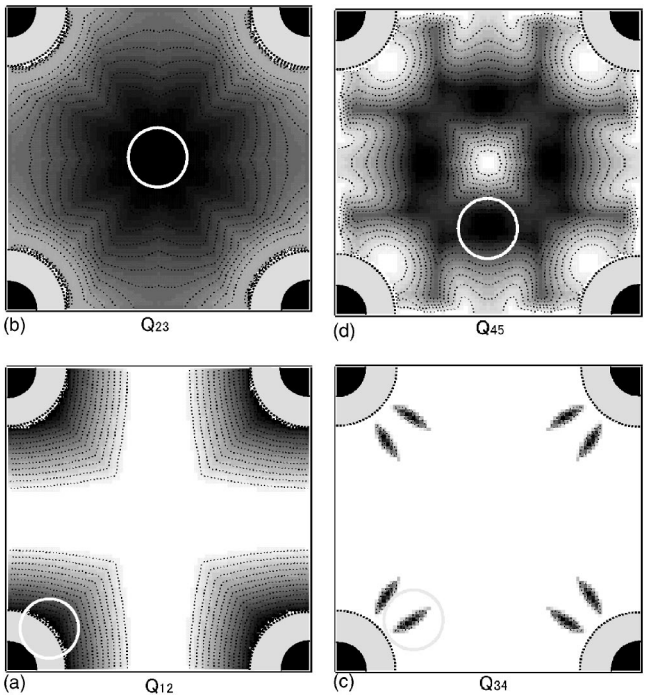

FIG. 2. Contours of the quality factor Q_{ij} (see text for its definition) for the photonic band gap between bands i and j as a function of the position of the second rod atom in the unit cell of the square lattice in two-dimensional binary-compound PCs. These figures correspond to the band gaps between bands (a) 1 and 2 (Q_{12}), (b) 2 and 3 (Q_{23}), (c) 3 and 4 (Q_{34}), and (d) 4 and 5 (Q_{45}). The brightest area indicates $Q_{ij}=0$, that is, no band gap, and the Q_{ij} value increases as the shade gets darker. The first atom is shown by the four closed quarter circles on the corners. The open circle indicates the second-atom position that maximizes the Q_{ij} value. In the gray area, there are no data of Q_{ij} since the second atom is not allowed to be placed in this area to avoid the overlap between atoms.

Starting with the first kind of PC mentioned above (a single rod atom with $\varepsilon_{a1}=10$ and $R_1=0.1a$), we consider what occurs by adding a second atom with $\varepsilon_{a2}=15$ and $R_2=0.1a$ at an arbitrary position in the unit cell of the above PC. In the following paragraphs, we investigate how the band structures and the band gaps are evolved by carefully tuning the second-atom position. Our primary purpose is to clarify the variations of the quality factor Q_{ij} between bands i and j as a function of the position of the second rod atom in the binary-compound PC.

Figure 2 shows the contours of the quality factor, which displays the Q_{ij} level for the second-atom center being located at a point in the unit cell of the square lattice (i.e., the large square in Fig. 2). The results for the band gap between the first (1) and second (2) bands are shown in Fig. 2(a), and, in a similar manner, those between bands 2 and 3, bands 3 and 4, and bands 4 and 5 are shown in Figs. 2(b), 2(c), and 2(d), respectively. The dark quarter circles on the four corners are the first rod atoms, and the gray zones are the dead areas where the second-atom center cannot exist to avoid the overlap between the two rods. In the brightest regions, no band gaps open, i.e., $Q_{ij}=0$. The Q_{ij} level increases as the

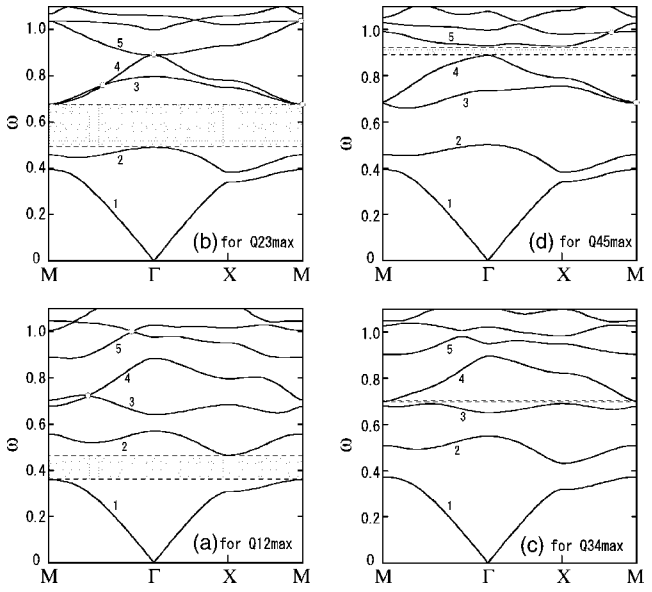

FIG. 3. Photonic band structures of the PCs with the second atoms indicated by open circles in Fig. 2. Hence, these figures shown by (a), (b), (c), and (d) correspond to those same symbols in Fig. 2. Open circles indicate the degenerate points (only points which bands 1 to 6 are involved in are shown). The angular frequency ω is normalized in units of $2\pi c/a$.

shade gets darker, i.e., the band gaps open ($Q_{ij}>0$) for these tones. Here, the second atoms can be considered everywhere in the unit cell, but those indicated by open circles are the second-atom positions which exhibit the maximum Q_{ij} level and moreover are the closest to the lower-left lattice points. The photonic band structures for these optimized configurations are shown in Fig. 3.

Let us first look at Fig. 2(a) for the Q_{12} contours. As shown in Fig. 2(a), the Q_{12} factor reaches a maximum (0.27) for the configuration in which the second atom contacts with the first one, which occurs at four equivalent positions in the unit cell. This configuration may be virtually regarded as a single atom with the increased radius and dielectric constant. Since the light waves involved in the formation of the lowest band gap are primarily those of wavelength $\lambda \sim 2a$, the simplest configuration like this may work best to create the 1-2 band gap. As the second atom becomes more distant from the lattice points, the Q_{12} factor decreases and finally disappears near the central region of the unit cell. Introducing the second atom near the central region is thus known to eliminate the 1-2 band gap, which was open in the absence of the second atom (though it was narrow, see the solid lines in Fig. 1). Therefore, we must unfortunately conclude that, for the formation of the 1-2 band gap, the introduction of the second atom is not very effective, but the optimization of the single atom may rather work better. This phenomenon will be discussed later in connection with the results in Fig. 2(b). Figure 3(a) shows the band structure for the PC with the maximum Q_{12}. The introduction of the second atom at the position shown by an open circle in Fig. 2(a) reduces the symmetry operations of this PC to (E, σ_d'). This symmetry reduction lifts the degeneracy at Γ and M points and newly opens the 2-3 band gap.

Figure 2(b) shows the Q_{23} contours for the 2-3 band gap. As we see dark patterns throughout this figure, this band gap is always generated for any positions of the second atom in the unit cell. This is in great contrast to the PC with a single atom (Fig. 1), which did not give a glimpse of the gap between bands 2 and 3. Considering that, as remarked before, the single-atom PC did not produce the 2-3 band gap for any combinations of dielectric constants and filling factors, we should mention that this band gap is generated for the first time by employing binary-compound PCs. The Q_{23} value increases, contrary to Q_{12}, as the second atom becomes distant from the first one, and it reaches the maximum at the center of the unit cell. In this case, the maximum occurs only at this point and hence no other equivalent points. The maximum Q_{23} value is estimated at 0.32, which is higher than that obtained for Q_{12}. The band structure of this PC [Fig. 3(b)] shows the degeneracy at four points, because of the recovered same symmetry as that for the original single-atom PC. That the 2-3 band gap opens despite many degenerate points will be explained in the subsequent paragraph.

Here, we pay attention to the fact that Q_{12} vanishes while Q_{23} achieves the maximum for the configuration that locates the second atom at the unit cell center. Note that the first and second atoms used here are similar to each other because of the same radii though there is a difference in the dielectric constants. So let us assume for a while that the second atom is identical to the first one. The primitive lattice vectors of that PC are no more $\mathbf{a}_1=a(1,0)$ and $\mathbf{a}_2=a(0,1)$ defined before, but $\mathbf{a}_1'=(\mathbf{a}_1-\mathbf{a}_2)/2$ and $\mathbf{a}_2'=(\mathbf{a}_1+\mathbf{a}_2)/2$. In other words, the unit cell of the square lattice is shrunk into the one defined by $\mathbf{a}_1'$ and $\mathbf{a}_2'$ with the area reduction by a factor of 2. This implies that the Brillouin zone (BZ) for the new unit cell is enlarged by a factor of 2: We here call it the new BZ and the original one the old BZ. When the band diagram is depicted in the form folded in the old first BZ, its BZ edge (on the *X*-*M* line) does not create any band gaps since it is not the actual BZ edge but nothing other than a band point within the new first BZ. From this, we recognize that the 1-2 band gap disappears when we look at it in the old BZ. This effect, however, will not reveal itself in the distinct form in our PC since it has different rod atoms ($\varepsilon_{a1}=10$ and $\varepsilon_{a2}=15$). For this reason, bands 1 and 2 must not coincide perfectly on the *X*-*M* line (BZ edge), but come close to each other [see Fig. 3(b)] and hence no 1-2 band gap. We thus know that the 1-2 band gap does not open around the second-atom positions where the large 2-3 band gap is observed.

The results of the Q_{34} contours for the 3-4 band gap are shown in Fig. 2(c). The area creating this band gap is extremely confined: Only narrow regions near the dead zones are the positions of the second atom for this gap formation. The maximum Q_{34} occurs at the center of the small island with $Q_{34}=0.014$, which has eight equivalent positions in the unit cell. Although the Q_{34} value obtained is small, it comes to have a positive value for the first time by adding the second atom to the single-atom PC. We recognize no degenerate points in the photonic band diagram of this PC [Fig. 3(c)] because of the very asymmetric atomic configuration: only the identity operation (E) exists. Owing to this nondegeneracy, the band gaps between any bands are found to open. The created band gaps, however, are not very large

compared with those obtained for the former configurations. This suggests that the mere reduction of the symmetry and the resultant lifting of band degeneracies are not always effective to enlarge the band gaps.

The final results studied here are for the Q_{45} contours for the 4-5 band gap [Fig. 2(d)]. The positions maximizing the Q_{45} value (0.045) are given by four equivalent points in the unit cell (one of them is indicated by an open circle). See also Fig. 3(d), where the 4-5 band gap is shown to open due to the reduced symmetry operations (E, σ_y) for this PC. Figure 2(d) exhibits somewhat intricate patterns compared with those for the former three. This suggests that the band gaps of higher indices such as 4-5 are more sensitive to the second-atom position. The formation of band gaps of higher indices implies the involvement of light-wave harmonics of higher orders. The harmonics, the wavelengths of which are much shorter than the lattice constant a, may require us to minutely tune the second-scatterer positions for the bandgap formation.

In conclusion, we have investigated the effects of relative configurations of two different rod atoms on the formation of photonic band gaps for E-polarized light in two-dimensional binary-compound photonic crystals. The photonic band gaps between any bands are found to be tuned by placing the second atom at an appropriate position in the unit cell. In particular, by elaborately searching for the optimal position of the second atom, we succeeded in determining the atomic configurations that maximize the photonic band gaps. Since this method is valid for another polarization (H polarization) also, the combination of the studies for these two polarizations will facilitate the formation of absolute band gaps. We believe that this kind of approach will prove useful in designing photonic band gaps of a variety of photonic crystals.

[1] *Photonic Crystals*, edited by K. Busch, S. Lölkes, R. B. Wehrspohn, and H. Föll (Wiley-VCH, Weinheim, 2004).
[2] *Photonic Band Gaps and Localization*, edited by C. M. Soukoulis (Plenum Press, New York, 1993).
[3] S. Nojima, J. Appl. Phys. **90**, 545 (2001).
[4] See, for example, P. R. Villeneuve and M. Piché, Phys. Rev. B **46**, 4969 (1992).
[5] I. H. H. Zabel and D. Stroud, Phys. Rev. B **48**, 5004 (1993).
[6] Z.-Y. Li, B.-Y. Gu, and G.-Z. Yang, Phys. Rev. Lett. **81**, 2574 (1998).
[7] X. Zhang and Z.-Q. Zhang, Phys. Rev. B **61**, 9847 (2000).
[8] A. Moroz and C. Sommers, J. Phys.: Condens. Matter **11**, 997 (1999).
[9] D. Cassagne, C. Jouanin, and D. Bertho, Phys. Rev. B **53**, 7134 (1996).
[10] C. M. Anderson and K. P. Giapis, Phys. Rev. B **56**, 7313 (1997).
[11] N. Malkova, S. Kim, T. DiLazaro, and V. Gopalan, Phys. Rev. B **67**, 125203 (2003).
[12] T. Trifonov, L. F. Marsal, A. Rodríguez, J. Pallarès, and R. Alcubilla, Phys. Rev. B **69**, 235112 (2004).
[13] See, for example, S. Nojima, Jpn. J. Appl. Phys., Part 1 **37**, 6418 (1998).
[14] K. Sakoda, *Optical Properties of Photonic Crystals* (Springer-Verlag, Germany, 2001).